Supplementary data

Materials and methods

Reagents

Rabbit anti-mouse PGC7 antibody was raised against full length of mouse PGC7. Small-molecule G9a inhibitor BIX-01294 was purchased from Sigma (Sigma, B9311).

Electrophoretic Mobility Shift Assay

Oligonucleotide substrates were obtained from IDT and were purified by polyacrylamidegel electrophoresis (PAGE). The following oligonucleotides containing PGC7 binding motif were used, 5'-GAGTAAGATCATGCCACTG***CACTTCAGCCTGG***GCACAGAGTGAGGCTGGG-3'. 50-mer oligonucleotides were annealed at 1:1 molar ratio to its complementary oligonucleotides to generate the dsDNA and then radio-labelled with ^{32}P at the 5'-end. GST-PGC7, deletion mutants D9 or GST protein with increased concentrations, was incubated with 0.2 nM (molecules) radio-labelled DNA substrate for 2 hours at 4 °C in buffer D (20 mM HEPES-KOH (pH 7.9), 20 % glycerol (vol/vol), 0.2 mM EDTA, 0.1 M KCl, 0.5 mM PSMF, 1mM DTT) with 1.25 μg/μL Bovine serum albumin, 1 mM DTT, 5 mM MgCl2. The samples were resolved by electrophoresis on a 7.5 % polyacrylamide gel in TBE buffer for 70 minutes at 60 V. The gel was then dried and exposed to autoradiography film overnight.

293T cells treated with G9a inhibitor

Small-molecule G9a inhibitor BIX-01294 (Sigma, B9311) (47) was solved in DMSO and used to treat 293T cells for 48 h.

Cell lysis and extraction of chromatin fraction

293T or MEF cells were lysed with ice-cold NETN100 buffer (0.5% NP-40, 50 mM Tris-HCl pH 8.0, 2 mM EDTA and 100 mM NaCl) containing 10 mM NaF and 50 mM β-glycerophosphate. The soluble fractions were collected and directly subjected to Western blotting analysis with indicated antibodies. For acid extraction of chromatin fraction, insoluble pellets were resuspended in 0.2 N HCl; and then the acid was neutralized by 1 M Tris-HCl (pH 8.5) for further Western blotting analysis.

Supplementary figure legends

Figure S1. PGC7 interacts with TET3. (A) PGC7 interacts with TET3, but not DNMT1, DNMT3a or DNMT3b. Co-IP was performed in 293T cells. Flag-tagged TET3, DNMT1, DNMT3a and DNMT3b were expressed in 293T cells and examined with indicated antibodies. The whole cell lysates (WCL) was used as the input. (B) PGC7 directly binds TET3. Sf9 cells were infected with baculoviruses encoding SBP-TET3CD and/or GST-PGC7. The protein complex was purified by streptavidin beads or GST beads and examined by coomassie blue staining.

Figure S2. PGC7 suppresses the enzymatic activity of TET2 or TET3 *in vitro*. (A) PGC7 suppresses the enzymatic activity of TET3 *in vitro* in a dose-dependent manner. The *in vitro* 5hmC assays were performed and described in Material and Methods. 1 μg, 2.5 μg and 5 μg recombinant PGC7 were used to suppress TET3 for 5mC to 5hmC conversion *in vitro*. (B) GST-tagged wild type recombinant PGC7 or PGC7 mutant proteins were purified from Sf9 insect cells and used for *in vitro* assay. The proteins were purified by GST beads and examined by coomassie blue staining.

Figure S3. PGC7 suppresses the enzymatic activity of TET2CD and TET3CD *in vivo*. (A) 293T-PGC7 cells stably expressing SBP-PGC7 were established and used for *in vivo* experiments. Both endogenous and exogenous PGC7 were detected by anti-PGC7 antibody. Exogenous PGC7 expression is higher than endogenous PGC7 in 293T-PGC7 cells. (B) PGC7 suppresses the enzymatic activity of TET2CD and TET3CD *in vivo*. Immunofluorescence staining shows that TET3CD-induced 5hmC is suppressed by wild

type PGC7 in 293T-PGC7 cells. High transfection efficiency of TET3CD in 293T cells was shown.

Figure S4. PGC7 protects CpG methylation from TET3-induced DNA demethylation at imprinting loci. (A) Low-expression of TET2 and TET3 in HBL100 cells. IP-Western blotting results show the low expression level of endogenous TET2 and TET3 in HBL100 cells compared with that in 293T cells. β-actin was used as protein loading control. (B) Global 5mC level was examined by dot blotting assays in the presence or absence of PGC7 depletion and/or TET3 overexpression in HBL100 cells. TET3 overexpression leads to the loss of global 5mC level in HBL100 cells. (C) In the presence or absence of PGC7 depletion and/or TET3 overexpression, qRT-PCR was performed to examine the mRNA levels of imprinting genes *Peg1, Peg3, Peg10* and *H19* in HBL100 cells. Only in the presence of PGC7 depletion, TET3 overexpression leads to the increase of transcription of the imprinting genes *Peg1, Peg3, Peg10* and *H19* in HBL100 cells, suggesting the DNA methylation in these gene loci was protected by PGC7.

Figure S5. Colocalization of PGC7 and TET3 at a set of imprinting loci. ChIP-qPCR results indicate the colocalization of PGC7 and TET3 at *Peg1*, *Peg3*, *Peg10* and *H19* loci in HBL100 cells stably expressing TET3 or the D9 mutant of PGC7. Irrelevant IgG was used as control.

Figure S6. Analysis of ChIP-Seq results. (A) ChIP-Seq results were validated by ChIP-qPCR. ChIP-Seq fragment densities of TET3 (x-axis) are plotted against ChIP-qPCR fold-enrichment of TET3 (percentage ofinput) (y-axis) at 30 selected loci in 293T cells that represent a broad range of ChIP-Seq fragment counts. The 30 selected loci contain 10 loci that are TET3 positive (ChIP-Seqsignal >5), 10 loci that are PGC7, TET3 and 5mC positive, and the other 10 loci are TET3 negative. The same methods were used to analyze the ChIP-Seq result of PGC7 and MeDIP-Seq result. 20 loci identified as significantly enriched by ChIP-Seq were clearly differentiated from 10 unenriched loci in the plots. (B) DNA binding motif of PGC7 concluded from ChIP-Seq result was validated by Electrophoretic Mobility Shift Assay (EMSA). Recombinant PGC7 or PGC7 mutant proteins was incubated with ^{32}P-labelled 50 mer sequence motif-contained DNA oligonucleotides. Both wild type and D9 mutant proteins could bind to the DNA containing sequence motif. GST protein was used as control. (C) Gene ontology analysis of the target genes of TET3 and PGC7. Genes co-occupied by TET3 and PGC7 at promoter and gene body region (from -5 kb of transcription start site to +5 kb of transcription end site was submitted to Panther Website for geneontology analysis. The result was shown in pie diagram.

Figure S7. The variable regions inside of the TET2 and TET3 catalytic domains alone do not bind PGC7. The Flag-tagged variable region of the TET2 catalytic domain (TET2V) (a.a. 1420 to 1861 of TET2) was generated and expressed in 293T cells. Co-IP assays were performed with indicated antibodies. PGC7 did not interact with TET2V. Similarly, PGC7 did not interact with variable region of the TET3 catalytic domain

(TET3V) (a.a. 980 to 1518 of TET3). Flag-tagged TET2 catalytic domain (TET2CD) and TET2 catalytic domain (TET3CD) were used as positive controls.

Figure S8. PGC7 does not interact with OGT. Co-IP was performed in 293T cells. Flag-tagged OGT was expressed in 293T cells and examined with indicated antibodies. The whole cell lysates (WCL) was used as the input. Interaction with TET3 was used as positive control.

Figure S9. PGC7 is associated with the chromatin in the G9a inhibitor-treated 293T cells and SUV39H1/H2-double-deficient MEFs. (A) PGC7 in the chromatin and soluble fractions was examined by Western blotting in G9a inhibitor-treated 293T cells. Global H3K9me2 level was significantly reduced in BIX-01294-treated 293T cells. The chromatin-associated PGC7 was mildly reduced in BIX-01294-treated 293T cells compared with that in the untreated 293T cells. A significant portion of chromatin-associated PGC7 could still be detected in the BIX-01294-treated 293T cells. (B) PGC7 proteins in chromatin and soluble fraction were examined by Western blotting in SUV39H1/H2-double-deficient MEFs. Global H3K9me2 level was markedly decreased in SUV39H1/H2-double-deficient MEFs compared with that in wild type MEFs. The chromatin-associated PGC7 was only mildly decreased in the SUV39H1/H2-double-deficient MEFs. (C-D) The occupancy of PGC7 at *Peg1* and *H19* loci was examined by ChIP-qPCR in BIX-01294-treated or untreated 293T cells. Mild decrease of PGC7 at the imprinting loci was observed. Irrelevant IgG was used as control. PCR primers for human

imprinting gene loci were listed in Table S1. (E-F) PGC7 occupancy at the *Peg1* and *H19* loci was examined by ChIP-PCR in wild type or SUV39H1/H2-double-deficient MEFs.

Fig. S1

A

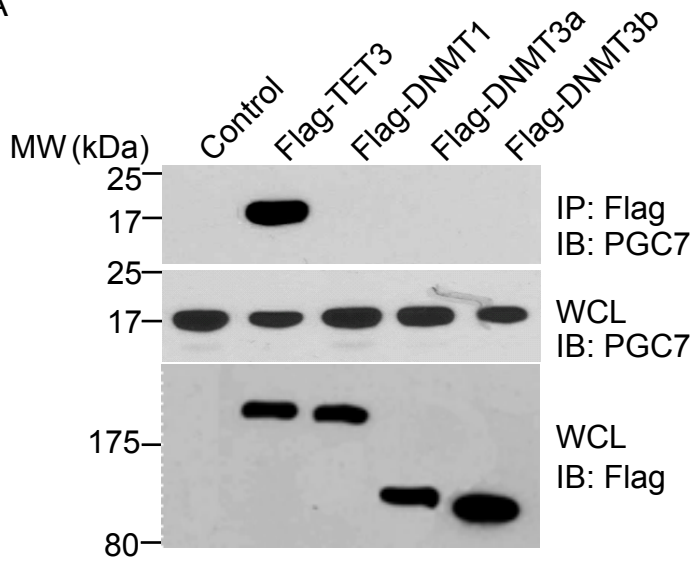

B

SBP-TET3CD	-	+	+	+	+
GST-PGC7	+	+	+	+	-
Stredavidin Beads	-	+	+	-	+
GST Beads	+	+	-	+	-

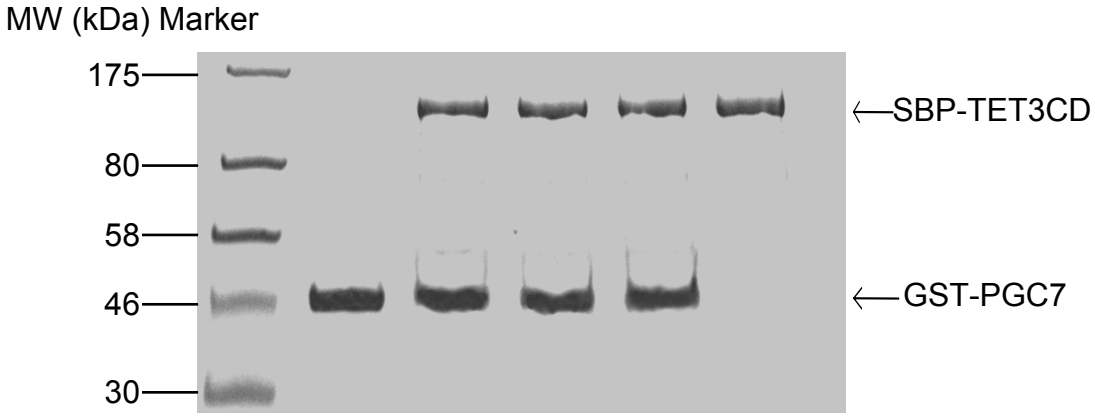

Fig. S2

A

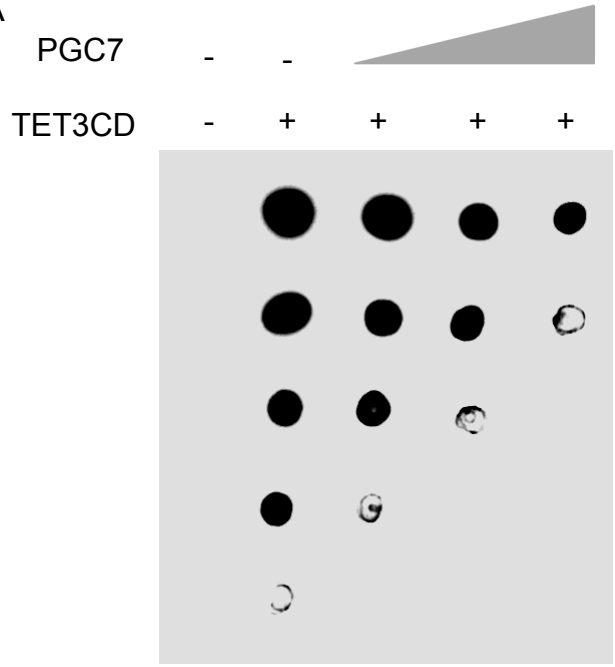
PGC7
- -
TET3CD
- + + + +
anti-5hmC

B

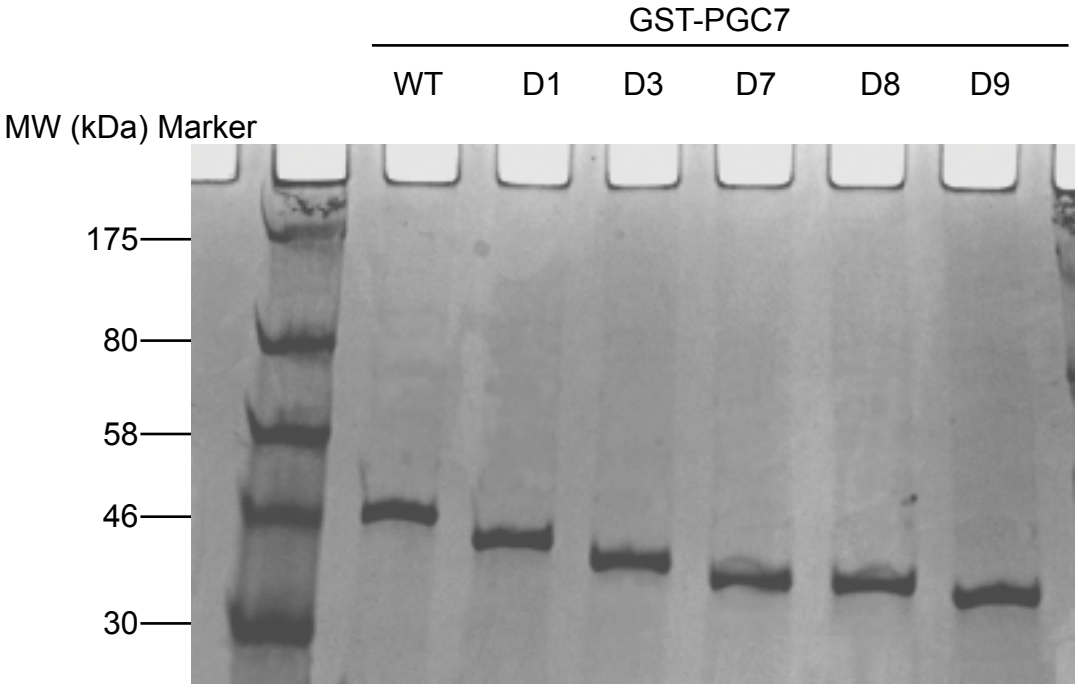
GST-PGC7
WT D1 D3 D7 D8 D9
MW (kDa) Marker
175
80
58
46
30

Fig. S3

A

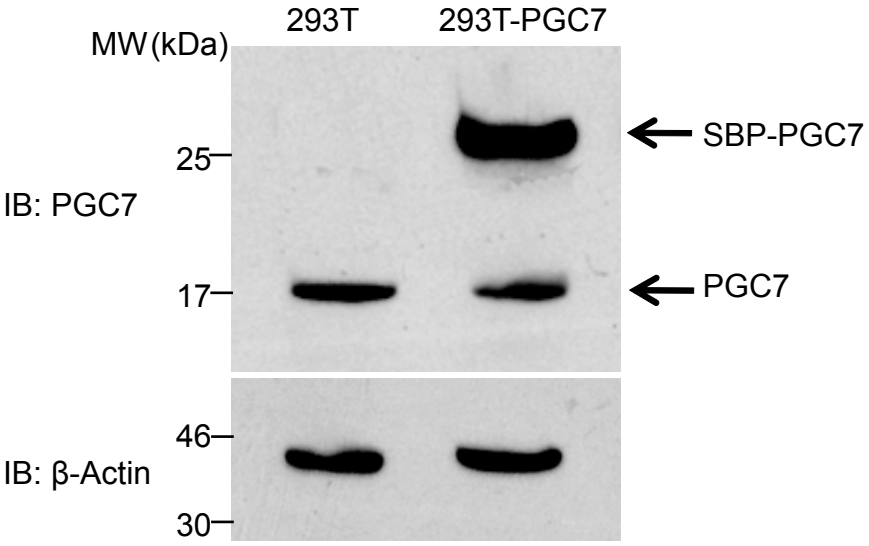
293T
293T-PGC7
MW (kDa)
25
17
IB: PGC7
SBP-PGC7
PGC7
46
30
IB: β-Actin

B

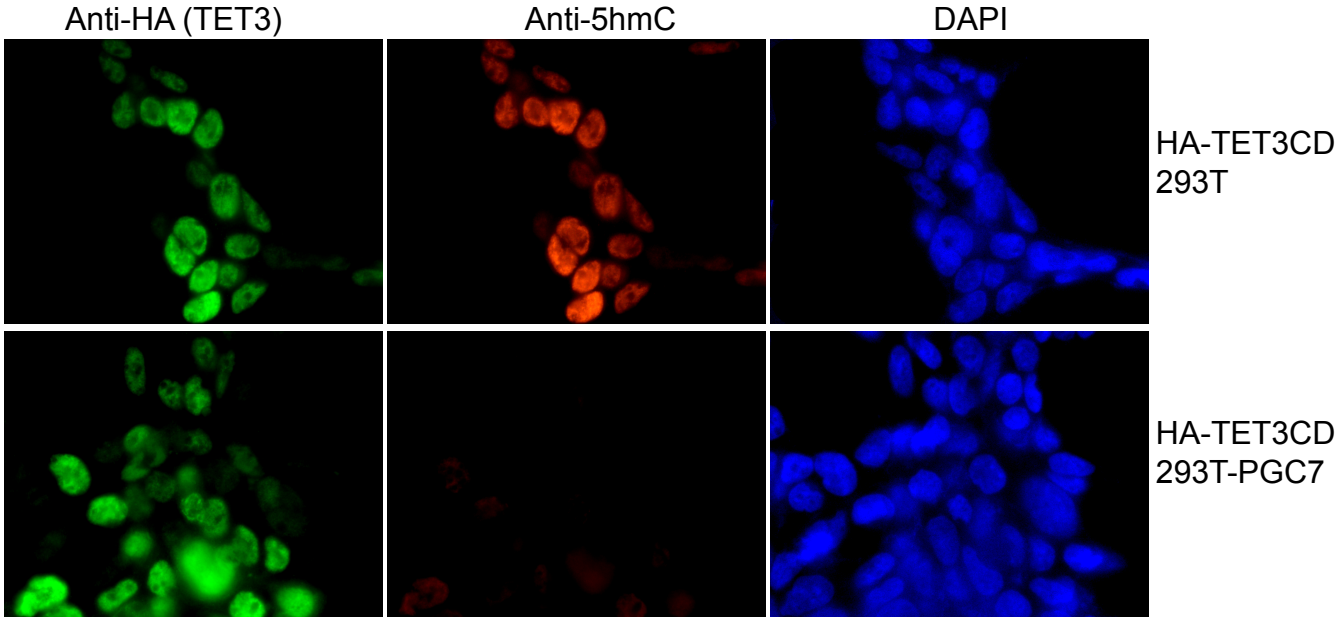
Anti-HA (TET3)
Anti-5hmC
DAPI
HA-TET3CD
293T
HA-TET3CD
293T-PGC7

Fig. S4

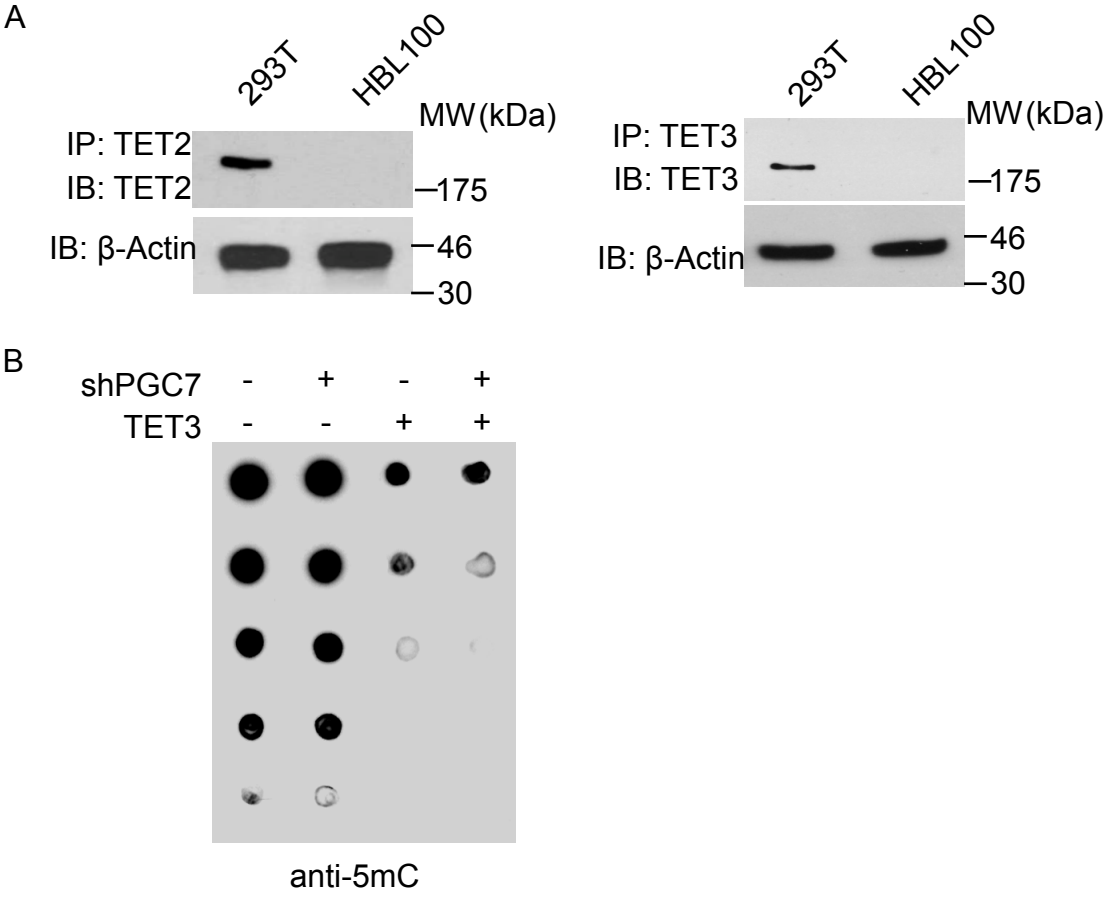
A
293T
HBL100
MW(kDa)
IP: TET2
IB: TET2
IB: β-Actin
175
46
30
293T
HBL100
MW(kDa)
IP: TET3
IB: TET3
IB: β-Actin
175
46
30
B
shPGC7 - + - +
TET3 - - + +
anti-5mC

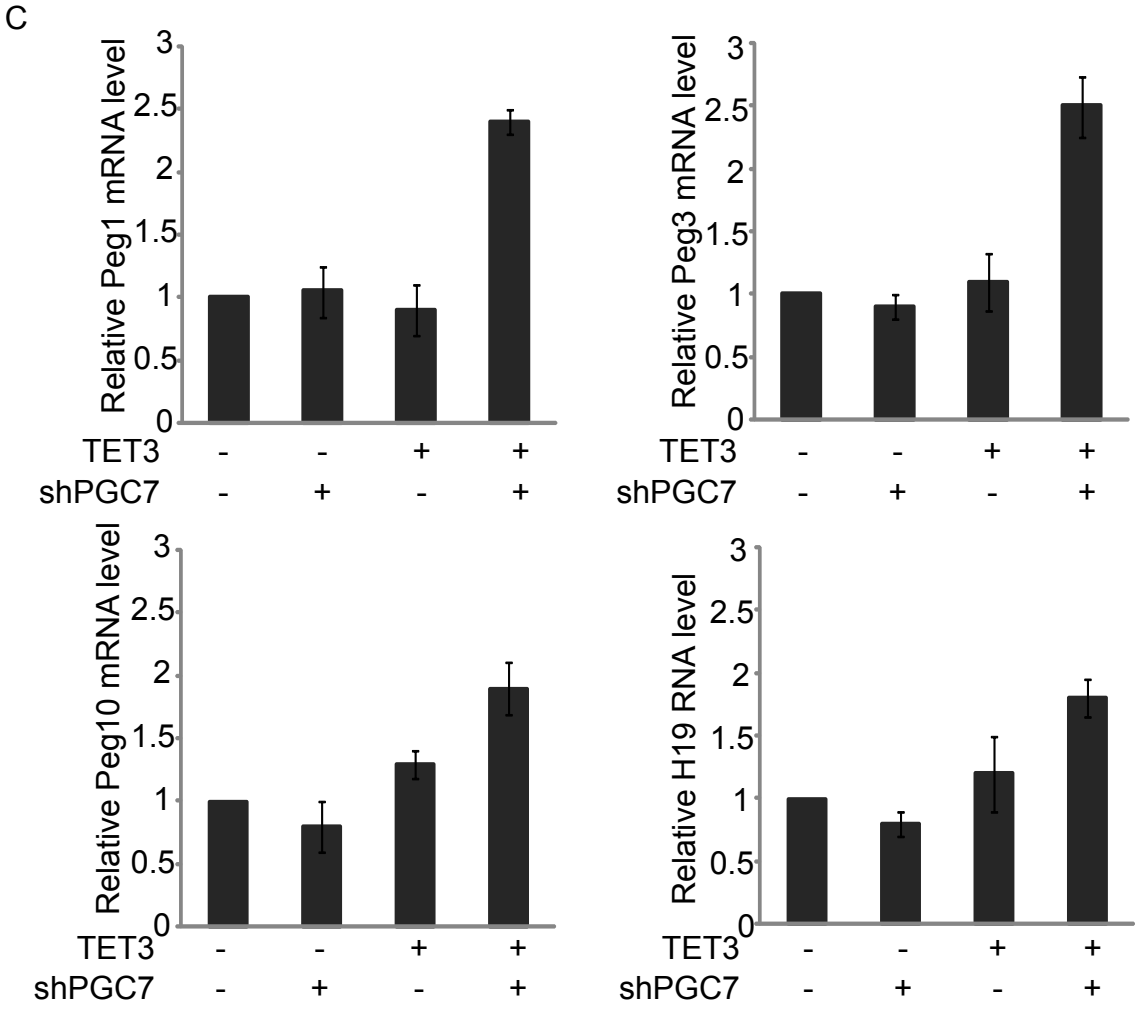
C
Relative Peg1 mRNA level
Relative Peg3 mRNA level
Relative Peg10 mRNA level
Relative H19 RNA level
0
0.5
1
1.5
2
2.5
3
TET3 - - + +
shPGC7 - + - +

Fig. S5

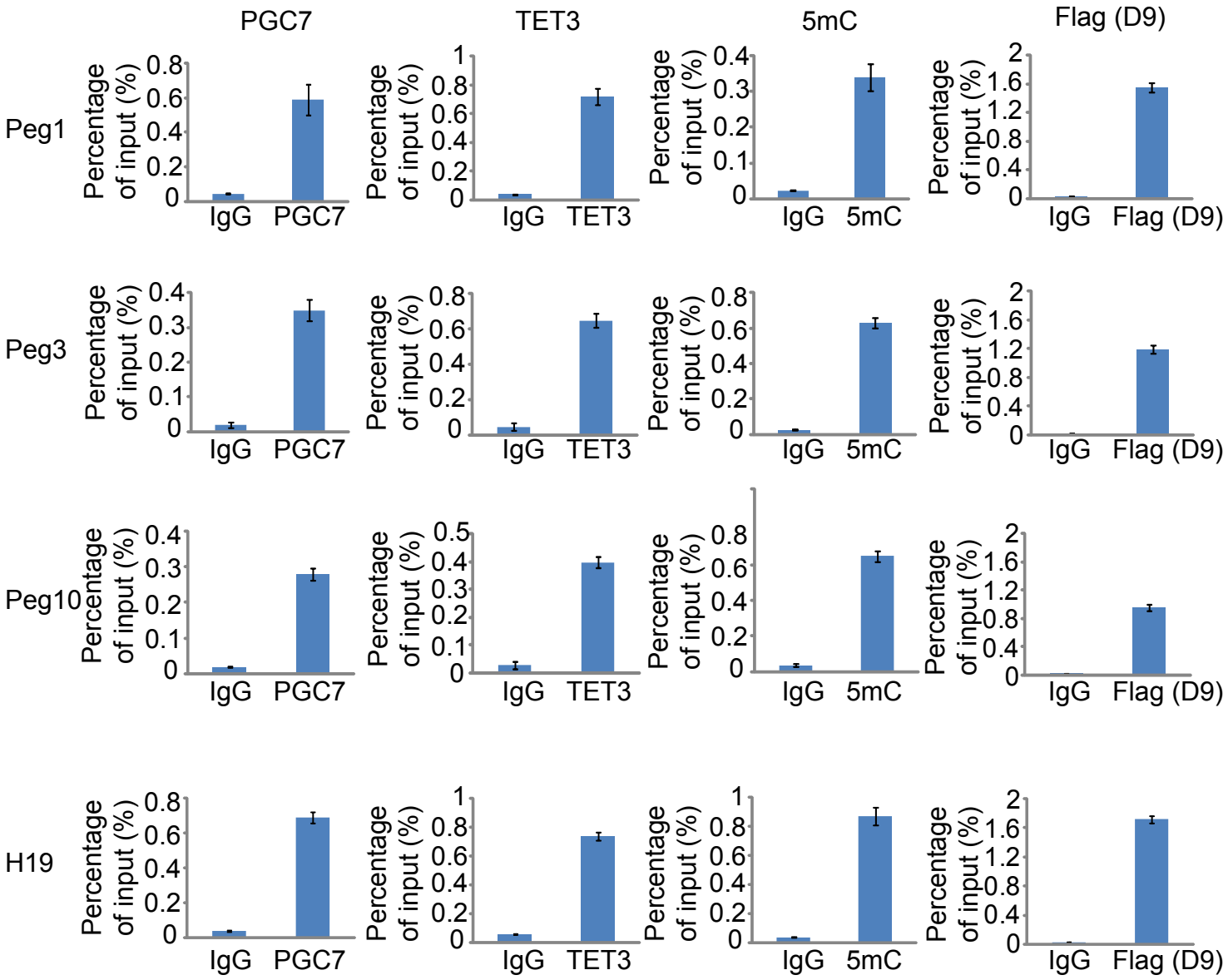
PGC7
TET3
5mC
Flag (D9)
Peg1
Peg3
Peg10
H19
Percentage of input (%)
IgG
PGC7
TET3
5mC
Flag (D9)

Fig. S6

A

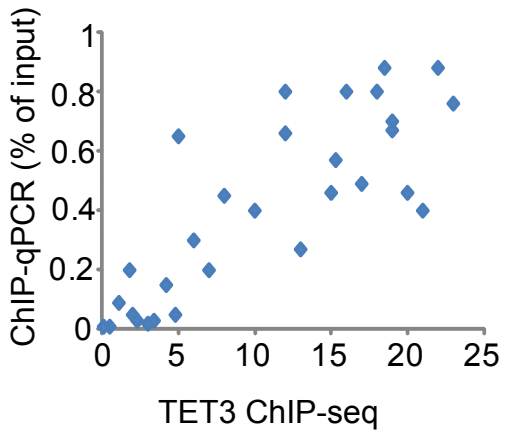
ChIP-qPCR (% of input)
1
0.8
0.6
0.4
0.2
0
0
5
10
15
20
25
TET3 ChIP-seq

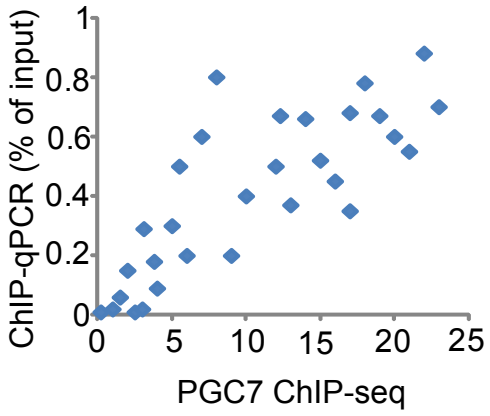
ChIP-qPCR (% of input)
1
0.8
0.6
0.4
0.2
0
0
5
10
15
20
25
PGC7 ChIP-seq

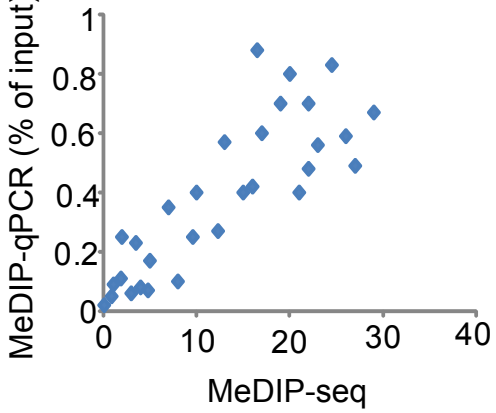
MeDIP-qPCR (% of input)
1
0.8
0.6
0.4
0.2
0
0
10
20
30
40
MeDIP-seq

B

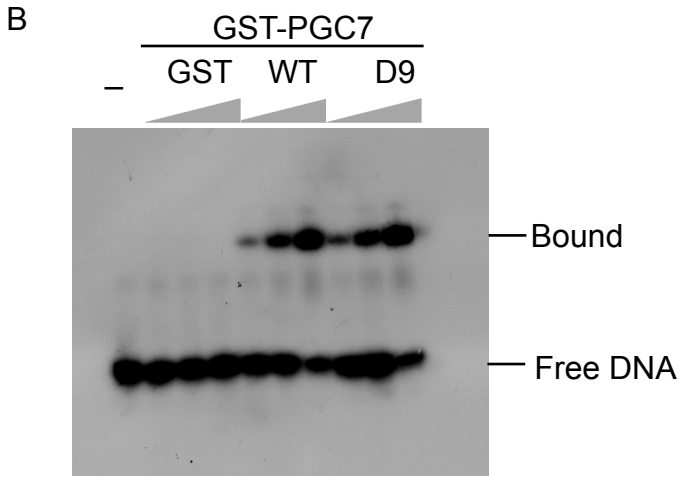
GST-PGC7
GST
WT
D9
–
Bound
Free DNA

C

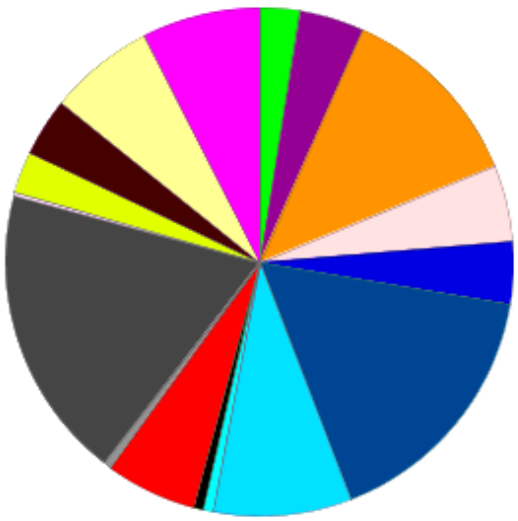

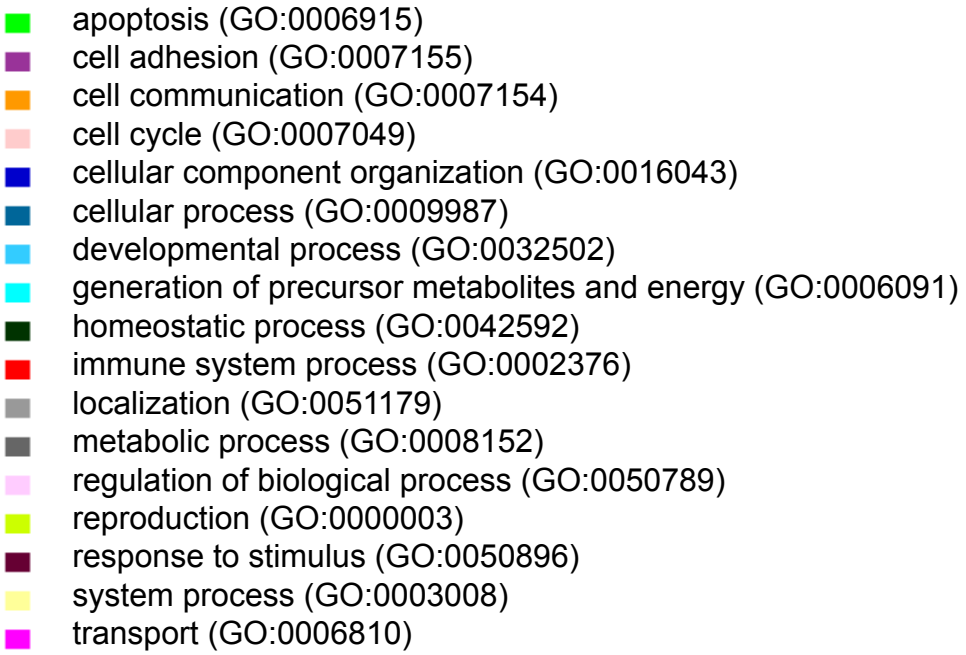
apoptosis (GO:0006915)
cell adhesion (GO:0007155)
cell communication (GO:0007154)
cell cycle (GO:0007049)
cellular component organization (GO:0016043)
cellular process (GO:0009987)
developmental process (GO:0032502)
generation of precursor metabolites and energy (GO:0006091)
homeostatic process (GO:0042592)
immune system process (GO:0002376)
localization (GO:0051179)
metabolic process (GO:0008152)
regulation of biological process (GO:0050789)
reproduction (GO:0000003)
response to stimulus (GO:0050896)
system process (GO:0003008)
transport (GO:0006810)

Fig. S7

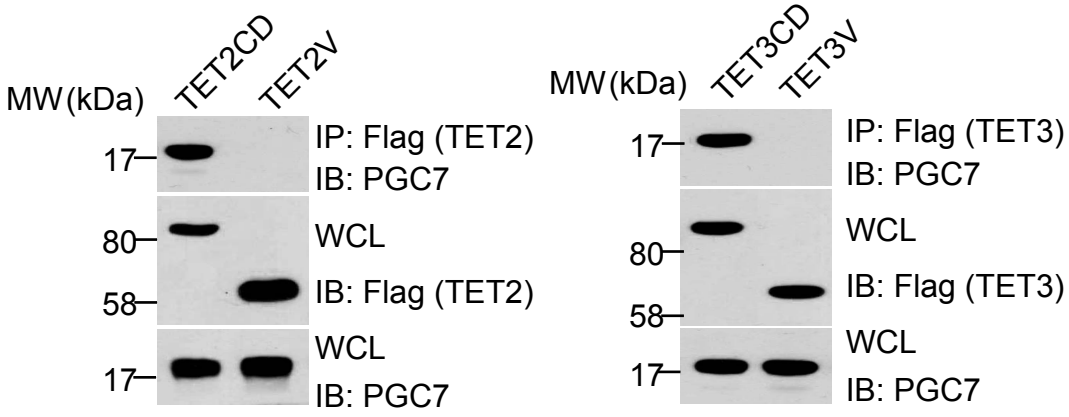
MW(kDa)
TET2CD
TET2V
17
IP: Flag (TET2)
IB: PGC7
80
58
WCL
IB: Flag (TET2)
17
WCL
IB: PGC7
MW(kDa)
TET3CD
TET3V
17
IP: Flag (TET3)
IB: PGC7
80
58
WCL
IB: Flag (TET3)
17
WCL
IB: PGC7

Fig. S8

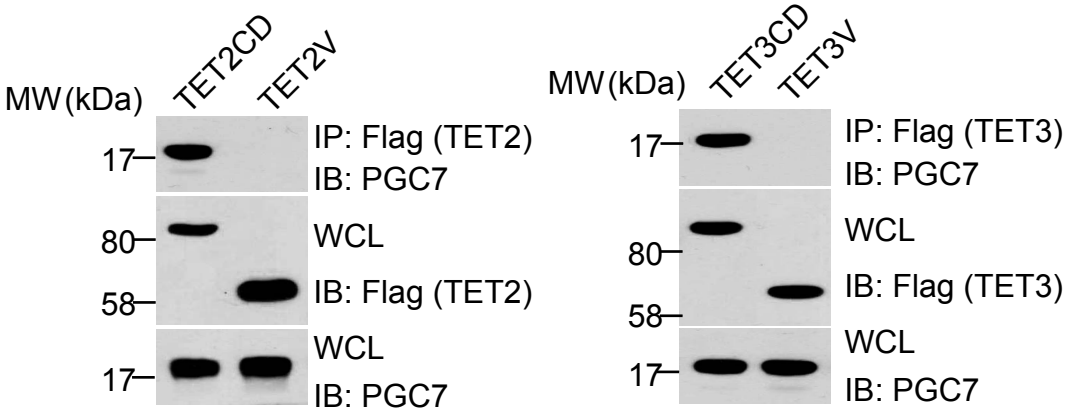
MW(kDa)
TET2CD
TET2V
17
IP: Flag (TET2)
IB: PGC7
80
WCL
58
IB: Flag (TET2)
17
WCL
IB: PGC7
MW(kDa)
TET3CD
TET3V
17
IP: Flag (TET3)
IB: PGC7
80
WCL
58
IB: Flag (TET3)
17
WCL
IB: PGC7

Fig. S9

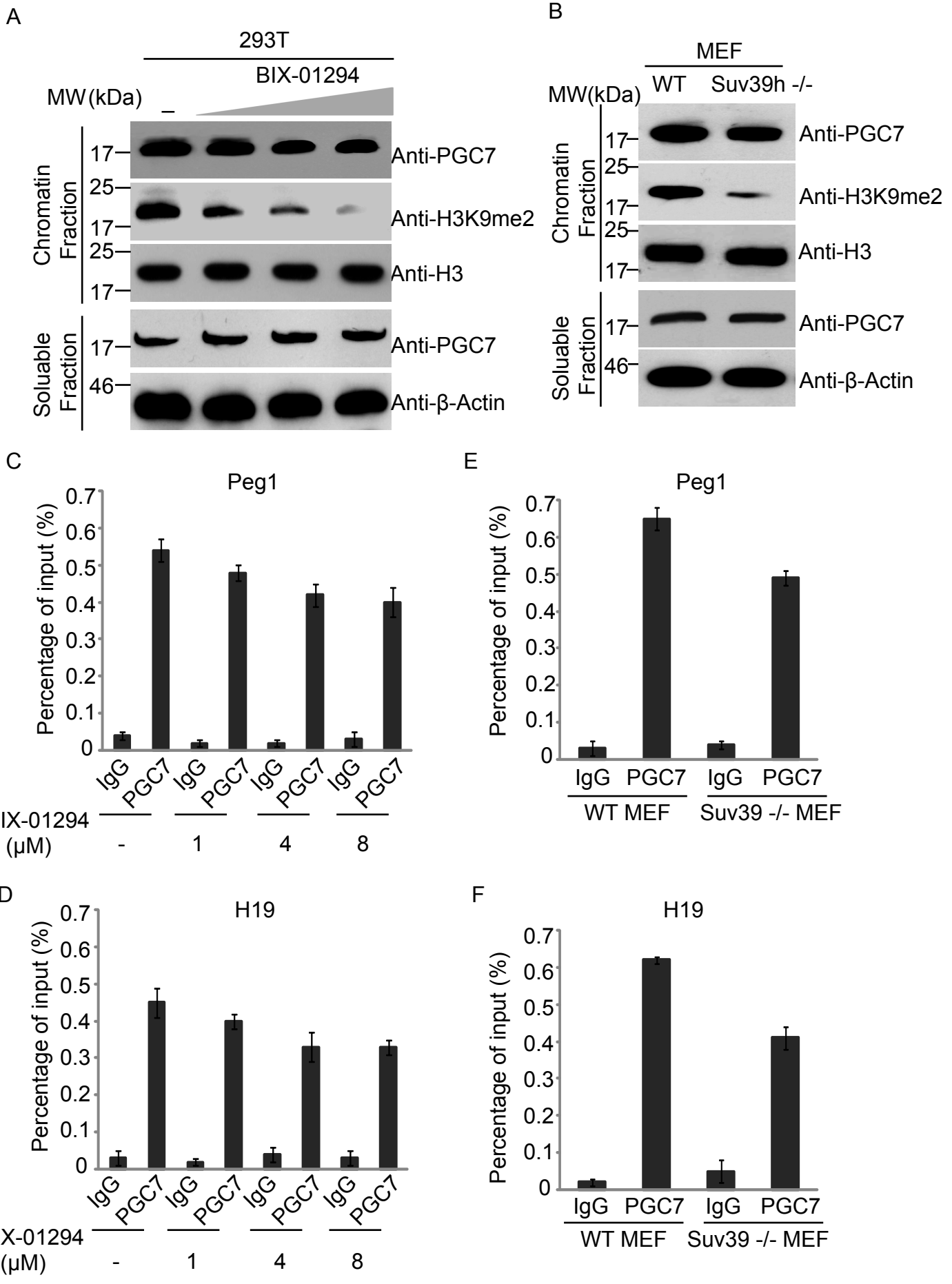
A
293T
BIX-01294
MW(kDa)
Chromatin Fraction
Soluable Fraction
17
25
17
25
17
17
46
Anti-PGC7
Anti-H3K9me2
Anti-H3
Anti-PGC7
Anti-β-Actin
B
MEF
WT
Suv39h -/-
MW(kDa)
Chromatin Fraction
Soluable Fraction
17
25
17
25
17
17
46
Anti-PGC7
Anti-H3K9me2
Anti-H3
Anti-PGC7
Anti-β-Actin
C
Peg1
Percentage of input (%)
0.7
0.6
0.5
0.4
0.3
0.2
0.1
0
IgG
PGC7
BIX-01294 (μM)
-
1
4
8
D
H19
Percentage of input (%)
BIX-01294 (μM)
E
Peg1
Percentage of input (%)
IgG
PGC7
WT MEF
Suv39 -/- MEF
F
H19
Percentage of input (%)